

## Observation of a metamagnetic transition in the $5f$ heavy-fermion compound $\text{UNi}_2\text{Al}_3$ : Magnetization studies up to 90 T for single-crystalline $\text{U}(\text{Pd}_{1-x}\text{Ni}_x)_2\text{Al}_3$

Kenji Mochizuki,<sup>1</sup> Yusei Shimizu,<sup>2,\*</sup> Akihiro Kondo,<sup>1</sup> Akira Matsuo,<sup>1</sup> Dexin Li,<sup>2</sup> Dai Aoki,<sup>2,3</sup> Yoshiya Homma,<sup>2</sup> Fuminori Honda,<sup>2</sup> Jacques Flouquet,<sup>3</sup> Daisuke Nakamura,<sup>1</sup> Shojiro Takeyama,<sup>1</sup> and Koichi Kindo<sup>1</sup>

<sup>1</sup>*Institute for Solid State Physics, University of Tokyo, Kashiwa, Chiba 277-0885, Japan*

<sup>2</sup>*Institute for Materials Research, Tohoku University, Oarai, Ibaraki 311-1313, Japan*

<sup>3</sup>*Université Grenoble Alpes, INAC/PHELIQS, CEA-Grenoble, F-38000 Grenoble, France*



(Received 2 July 2018; revised manuscript received 6 September 2019; published 23 October 2019)

We report an observation of metamagnetism in the  $5f$ -electron heavy-fermion antiferromagnets  $\text{UNi}_2\text{Al}_3$  at 78 T and  $\text{U}(\text{Pd}_{1-x}\text{Ni}_x)_2\text{Al}_3$  at 30 T (42 T) for  $x = 0.5$  ( $x = 0.75$ ) using single-crystalline samples. The magnetization curves for  $\text{U}(\text{Pd}_{1-x}\text{Ni}_x)_2\text{Al}_3$  ( $x = 0.5$  and  $0.75$ ) show a sharp increase at the metamagnetic transition (MMT) field  $B_m$ , strongly indicating their first-order nature. The obtained  $B$ - $T$  phase diagram for  $x = 0.5$  suggests the possible presence of the tricritical point, while the MMT still occurs at high temperatures above  $T_N$  from paramagnetic to polarized-paramagnetic states as a crossover. The results indicate that the antiferromagnetic order is closely connected to the MMT in  $\text{U}(\text{Pd}_{1-x}\text{Ni}_x)_2\text{Al}_3$ , but the metamagnetic behavior cannot be explained by the conventional spin flip of antiferromagnetic ordered moments. Our data for  $\text{U}(\text{Pd}_{1-x}\text{Ni}_x)_2\text{Al}_3$  have revealed an empirical linear relation of  $B_m(x) \propto T_{\chi_{\max}}(x)$  and a scaling behavior in magnetic susceptibility of  $\chi(T/T_{\chi_{\max}})/\chi_{\max}$ , where  $T_{\chi_{\max}}$  is the temperature of the susceptibility maximum [ $\chi_{\max} \equiv \chi(T_{\chi_{\max}})$ ]. Importantly, the critical value of the magnetic polarization at the MMT  $M_{\text{cr}}$  is roughly unchanged, although the value of susceptibility is notably suppressed with increasing  $x$ .

DOI: [10.1103/PhysRevB.100.165137](https://doi.org/10.1103/PhysRevB.100.165137)

### I. INTRODUCTION

The metamagnetic transition (MMT) has been extensively studied to describe the first-order spin-flipping transition in localized antiferromagnets with a strong anisotropy [1]. Subsequently, itinerant electron systems were also found to exhibit MMT, reflecting ferromagnetic (FM) instabilities and/or a change of Fermi-surface topology (Lifshitz transition). So far the itinerant MMT has been extensively studied on  $d$ - and  $f$ -electron systems. For instance, the MMT in  $d$ -electron  $\text{Y}(\text{Co}, \text{Al})_2$  [2,3] is explained by band magnetism, associated with the Stoner instability [4] and spin-fluctuation effects [5]. Recently, the itinerant MMT was extensively studied for the strongly correlated  $d$ -electron metallic system  $\text{Sr}_3\text{Ru}_2\text{O}_7$ , which exhibits a pressure-induced FM quantum criticality [6–10]. Interestingly, novel phases have been observed around the itinerant MMT, accompanied by the Fermi-surface distortion [8], and the MMT has been explained by the presence of the so-called FM wing structure [9]. In the case of  $f$ -electron heavy-fermion systems, possessing the dual nature of  $f$  electrons (itinerant and localized characteristics), there is no systematic understanding of the MMT despite the numerous studies reported so far. The understanding of the origin of the MMT has become increasingly important, as novel phenomena accompanied by MMTs have been observed in strongly correlated electron systems. Recently, it was found that a spin-density-wave state emerges along with the successive MMTs near the boundary of the hidden-ordered phase

in  $\text{URu}_2\text{Si}_2$  [11–13], whose undefined order parameter has been intensively debated for more than three decades [14]. Moreover, very recently, the first-order MMT was discovered at  $B_m = 35$  T in the novel heavy-fermion superconductor  $\text{UTe}_2$  [15,16], associated with the field-reentrant superconductivity near  $B_m$ , indicating close interplay between the MMT and unconventional Cooper pairing in strongly correlated  $5f$  electrons [17–20].

One of the most typical heavy-fermion metamagnets is  $\text{CeRu}_2\text{Si}_2$ , which has a tetragonal crystal structure with a strong Ising-type anisotropy, that is,  $\chi_{\max}^{H\parallel c}/\chi_{\max}^{H\perp c} \approx 15$  at  $T_{\chi_{\max}}$  of 10 K [21]. In  $\text{CeRu}_2\text{Si}_2$ , the pseudo-MMT occurs at 7.8 T as a crossover anomaly, marked by a sharp effective mass enhancement [21–24]. In this paramagnetic (PM) system, it has been discussed that the MMT is caused by the itinerant-to-localized crossover [21–25] or its dramatic change of Fermi surface, leading to a Lifshitz transition [25–27]. As shown by several studies for pure  $\text{CeRu}_2\text{Si}_2$  and its doped systems  $\text{Ce}_{1-x}\text{La}_x\text{Ru}_2\text{Si}_2$  [28,29] and  $\text{Ce}(\text{Ru}_{1-x}\text{Rh}_x)_2\text{Si}_2$  [30], competitive antiferromagnetic (AF) correlations and field-induced ferromagnetism play a key role in the MMT in  $\text{CeRu}_2\text{Si}_2$  [31,32]. For  $5f$ -electron systems, the MMT has been observed in  $\text{URu}_2\text{Si}_2$  [11,12,33],  $\text{UPt}_3$  [34],  $\text{UPd}_2\text{Al}_3$  [35–37],  $\text{UCoAl}$  [38], and  $\text{UTe}_2$  [17–19]. In the case of  $\text{UCoAl}$ , the MMT is observed at the weak magnetic field of 0.6 T [38], and it has been understood that the MMT occurs owing to the first-order wing structure in the vicinity of the FM quantum phase transition [39–42]. For the other uranium systems, little is known about the mechanism of the MMT phenomena that are seen in high-magnetic fields. It is therefore of interest to investigate the interplay between the

\*yuseishimizu@imr.tohoku.ac.jp

magnetic order and MMT in the magnetic phase diagram in  $5f$  heavy-fermion systems.

Our targets in the present paper are the isostructural  $\text{UPd}_2\text{Al}_3$  and  $\text{UNi}_2\text{Al}_3$ , both of which crystallize in a hexagonal  $\text{PrNi}_2\text{Al}_3$ -type structure. Interestingly, these two systems show the coexistence of antiferromagnetism and unconventional superconductivity [43,44].  $\text{UPd}_2\text{Al}_3$  undergoes an AF order with  $\mathbf{Q} = (0, 0, 1/2)$  of the ordered moment  $m_0 \sim 0.85 \mu_B/\text{U}$  at  $T_N \sim 14.5$  K [45,46], whereas  $\text{UNi}_2\text{Al}_3$  exhibits an incommensurate AF order at  $T_N \sim 4.5$  K possessing  $\mathbf{Q} = (1/2 \pm \tau, 0, 1/2)$  for  $m_0 \sim 0.2 \mu_B/\text{U}$ , with  $\tau \sim 0.11$  [47–49]. In  $\text{UPd}_2\text{Al}_3$ , the magnetic susceptibility  $\chi$  as a function of temperature  $\chi(T)$  shows a maximum at  $T_{\chi_{\max}} \sim 35$  K in the PM state [43]. Such a susceptibility maximum is frequently observed in systems showing a MMT, and there is an empirical linear relation between  $T_{\chi_{\max}}$  and the MMT field  $B_m$  in various compounds [2,3,50]. For  $\text{UPd}_2\text{Al}_3$ , it was previously reported that the MMT and the collapse of the AF state simultaneously occur at 18.5 T [37].  $\text{UNi}_2\text{Al}_3$  also shows a susceptibility maximum at  $T_{\chi_{\max}} \sim 105$  K, and hence, its large energy scale reminds us of the metamagnetic instability in a much higher field, where no MMT has been observed up to 35 T so far [51]. It is noted that both  $\text{UPd}_2\text{Al}_3$  and  $\text{UNi}_2\text{Al}_3$  exhibit the easy-plane type of magnetic anisotropy, and the susceptibility maximum is seen for easy-magnetization directions perpendicular to the hexagonal  $c$  axis [52,53]. The magnetic anisotropy at  $T_{\chi_{\max}}$  in  $\text{UNi}_2\text{Al}_3$  ( $\chi_{\max}^{H_{\perp c}}/\chi_{\max}^{H_{\parallel c}} \approx 3$ ) [52] is smaller than that for  $\text{UPd}_2\text{Al}_3$  ( $\chi_{\max}^{H_{\perp c}}/\chi_{\max}^{H_{\parallel c}} \approx 6$ ) [53,54].

To explore the MMT in  $\text{UNi}_2\text{Al}_3$ , we have performed high-resolution magnetization measurements for single-crystalline  $\text{UNi}_2\text{Al}_3$  and  $\text{U}(\text{Pd}_{1-x}\text{Ni}_x)_2\text{Al}_3$  in magnetic fields up to 90 T. In this paper, we report the observation of metamagnetism in  $\text{UNi}_2\text{Al}_3$  at 78 T. Additionally, as quantitative magnetization measurements under fields higher than 60 T are experimentally very difficult, we also performed detailed high-field magnetization measurements at various temperatures for the doped samples of  $x = 0.5$  and  $0.75$ , which are also found to exhibit the MMT at lower field strengths of 30 and 42 T, respectively.

## II. EXPERIMENTAL PROCEDURES

Single-crystalline  $\text{U}(\text{Pd}_{1-x}\text{Ni}_x)_2\text{Al}_3$  ( $x = 0, 0.3, 0.5, 0.75$ , and 1) samples were grown using the Czochralski pulling method in a tetra-arc furnace. The magnetic susceptibility was measured from 2 to 300 K by a magnetic properties measurement system (Quantum Design). The high-field  $M(B)$  measurements of  $\text{UNi}_2\text{Al}_3$  up to 75 T were performed using a nondestructive pulsed magnet with a duration of 4 ms, and another with a longer duration of 36 ms was used for  $M(B)$  measurements for  $\text{U}(\text{Pd}_{1-x}\text{Ni}_x)_2\text{Al}_3$  up to 49 T at low temperatures down to 1.4 K. Furthermore, magnetization of  $\text{UNi}_2\text{Al}_3$  was also measured in fields up to 90 T, using a single-turn coil in a destructive magnet at 4.2 K [55], where the absolute value of the magnetization could not be obtained for the metallic  $\text{UNi}_2\text{Al}_3$  owing to the experimental difficulty. Magnetic fields were applied along the easy-magnetization [1120] axis in the hexagonal basal plane. Here, the low-temperature physical properties of  $\text{UN}_2\text{Al}_3$  are strongly sample dependent [56]. Our sample of single-crystalline  $\text{UN}_2\text{Al}_3$  shows the AF transition

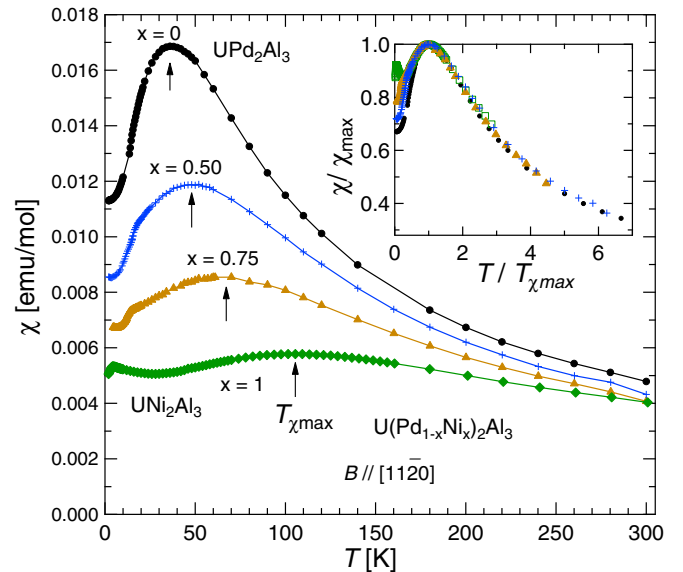


FIG. 1.  $\chi(T)$  in  $\text{U}(\text{Pd}_{1-x}\text{Ni}_x)_2\text{Al}_3$  ( $x = 0, 0.5, 0.75$ , and 1.0), measured at 0.5 T for  $B \parallel [11\bar{2}0]$ , where  $T_{\chi_{\max}}$  are indicated by arrows. Inset: The normalized susceptibility  $\chi(T)/\chi(T_{\chi_{\max}})$  as a function of  $T/T_{\chi_{\max}}$ .

at 4.1 K, which is slightly lower than the previously reported value for polycrystalline samples [56].

## III. RESULTS AND DISCUSSION

Figure 1 shows the magnetic susceptibility  $\chi(T) \equiv M/B$  of  $\text{U}(\text{Pd}_{1-x}\text{Ni}_x)_2\text{Al}_3$  ( $x = 0, 0.5, 0.75$ , and 1) in the temperature range of 2 to 300 K at 0.5 T for  $B \parallel [11\bar{2}0]$ . The  $\chi(T)$  curves in  $\text{U}(\text{Pd}_{1-x}\text{Ni}_x)_2\text{Al}_3$  show pronounced maxima in the PM state at temperature  $T_{\chi_{\max}}$ . Interestingly,  $T_{\chi_{\max}}$  shifts to higher  $T$ , and the susceptibility maximum  $\chi_{\max}$  becomes broader with increasing  $x$ . In  $\text{UNi}_2\text{Al}_3$ ,  $\chi(T)$  shows a local minimum at  $\sim 25$  K, and then  $\chi(T)$  increases upon cooling down to  $T_N$ . The inset of Fig. 1 shows the normalized magnetic susceptibility  $\chi(T)/\chi(T_{\chi_{\max}})$  as a function of  $T/T_{\chi_{\max}}$ . Interestingly,  $\chi(T)/\chi(T_{\chi_{\max}})$  for each  $x$  obeys the scaling behavior in the  $T$  range from  $0.8T_{\chi_{\max}}$  to  $7T_{\chi_{\max}}$ . This scaling of magnetic susceptibility implies that there is a similar effect of AF spin fluctuations in the isostructural system  $\text{U}(\text{Pd}_{1-x}\text{Ni}_x)_2\text{Al}_3$ . For  $\text{UNi}_2\text{Al}_3$ ,  $\chi(T)$  weakly enhances upon cooling down to  $T_N$ , suggesting the presence of another magnetic instability at low  $T$  below 30 K.

Figures 2(a) and 2(b) show  $M(B)$  curves for  $\text{U}(\text{Pd}_{1-x}\text{Ni}_x)_2\text{Al}_3$  ( $x = 0, 0.5, 0.75$ , and 1.0) along with their derivatives  $dM(B)/dB$ . For  $x = 0$ , the sharp MMT occurs at around 18.8 T [37]. Interestingly, the MMT is observed for  $\text{U}(\text{Pd}_{1-x}\text{Ni}_x)_2\text{Al}_3$ , and the MMT field  $B_m$  shifts to higher fields with increasing  $x$ . Here, we define  $B_m$  as the point at which the magnetization derivative shows a maximum. For  $\text{UNi}_2\text{Al}_3$ , the onset of metamagnetism is also observed in  $M(B)$  as well as its derivative [Fig. 2(b)] near 80 T. The inset shows the results of  $dM(B)/dB$  for  $\text{UNi}_2\text{Al}_3$  up to 90 T, using a destructive magnet [inset of Fig. 2(b)]. The maximum in  $dM(B)/dB$  strongly suggests the occurrence of the MMT around 78 T in  $\text{UNi}_2\text{Al}_3$ .

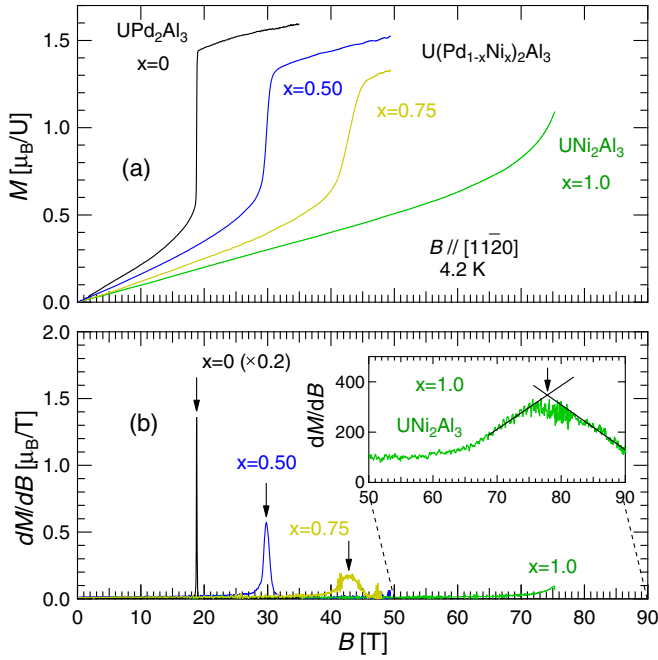


FIG. 2. (a) The  $M(B)$  curves of  $U(Pd_{1-x}Ni_x)_2Al_3$  ( $x = 0, 0.5, 0.75,$  and  $1.0$ ), measured at  $4.2$  K for  $B \parallel [11\bar{2}0]$ . (b) The derivative of the magnetization,  $dM(B)/dB$ , where the arrows indicate the MMT field  $B_m$ . Inset: The derivative of the magnetization measured in a destructive magnet.

Owing to the experimental difficulty of high-resolution magnetization measurements above  $70$  T, quantitative values of  $M(B)$  and the saturated moment in  $UNi_2Al_3$  are still unclear. Nevertheless, as shown in the inset of Fig. 2(b), the maximum in  $dM(B)/dB$  is clearly seen around  $78$  T, compared to the background, providing a strong indication of the MMT in  $UNi_2Al_3$ . In addition, as seen in the quantitative magnetization curve up to  $75$  T for  $UNi_2Al_3$ , there is a notable increase in magnetization (large nonlinear susceptibility) near the MMT, and the magnetization value reaches almost  $\sim 0.9\mu_B/U$  at  $70$  T [Fig. 2(a)]. The magnetization value of  $\sim 0.9\mu_B/U$  just below the MMT is significantly larger than the magnitude of the incommensurate AF ordered moments with a maximum amplitude of  $\sim 0.2\mu_B/U$  [47,48], suggesting that the high-field magnetization curve in  $UNi_2Al_3$  cannot be explained by spin flip of magnetic moments with  $\sim 0.2\mu_B/U$ .

Figure 3(a) summarizes  $T_{\chi_{\max}}(x)$ ,  $T_N(x)$ , and  $B_m(x)$  for  $U(Pd_{1-x}Ni_x)_2Al_3$  as a function of  $x$ . With increasing  $x$ ,  $T_N(x)$  shows a slight maximum around  $x = 0.5$ , which is then suppressed approaching the pure  $UNi_2Al_3$  ( $x = 1$ ). These results for  $T_N(x)$  for single-crystalline samples are in good agreement with previous studies on polycrystalline samples [57].  $T_{\chi_{\max}}(x)$  and  $B_m(x)$  increase with increasing  $x$ , unlike  $T_N(x)$ . Figure 3(b) shows  $B_m$  versus  $T_{\chi_{\max}}$  for  $U(Pd_{1-x}Ni_x)_2Al_3$  along with results for various itinerant  $4f$  and  $5f$  heavy-fermion metamagnets [50], indicating linear proportionality between  $B_m$  and  $T_{\chi_{\max}}$  in  $U(Pd_{1-x}Ni_x)_2Al_3$ .

Figures 4(a) and 4(b) show  $M(B)$  curves for  $U(Pd_{1-x}Ni_x)_2Al_3$  ( $x = 0.5$  and  $0.75$ ), measured at various temperatures for  $B \parallel [11\bar{2}0]$ . The very sharp increase in the  $M(B)$  curves at low temperatures provides a strong indication

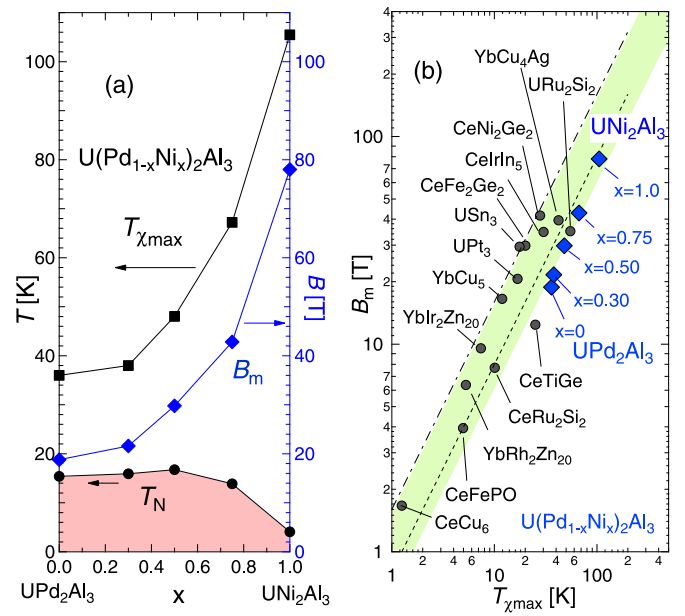


FIG. 3. (a)  $T_N(x)$ ,  $T_{\chi_{\max}}(x)$ , and  $B_m(x)$  for  $U(Pd_{1-x}Ni_x)_2Al_3$  as a function of  $x$ . (b) The logarithmic plot of  $B_m$  versus  $T_{\chi_{\max}}$  for  $U(Pd_{1-x}Ni_x)_2Al_3$  ( $x = 0, 0.30, 0.50, 0.75,$  and  $1.0$ ) along with results for various heavy-fermion itinerant metamagnets [50]. Here, the dash-dotted and dotted lines indicate  $B_m/T_{\chi_{\max}} = 1.6$  and  $= 0.8$ , respectively.

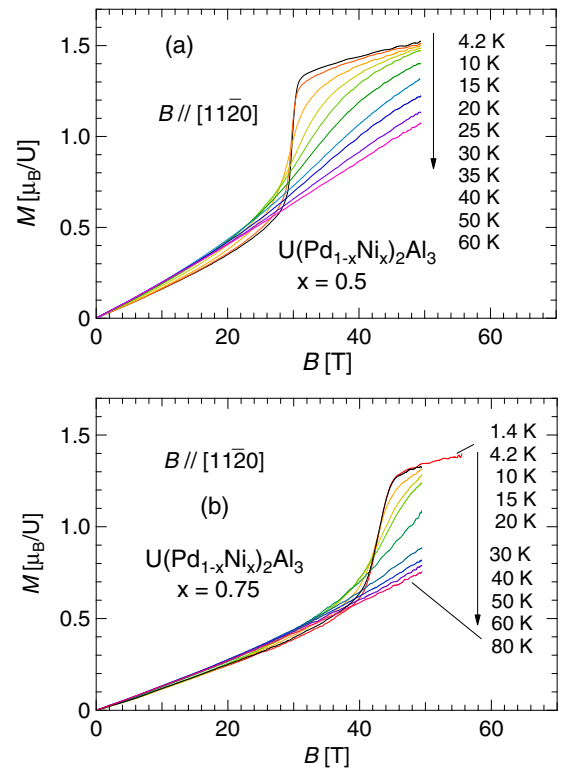


FIG. 4. The magnetization curves  $M(B)$  of  $U(Pd_{1-x}Ni_x)_2Al_3$  for (a)  $x = 0.5$  and (b)  $x = 0.75$  at various  $T$  along the easy-magnetization  $[11\bar{2}0]$  axis.

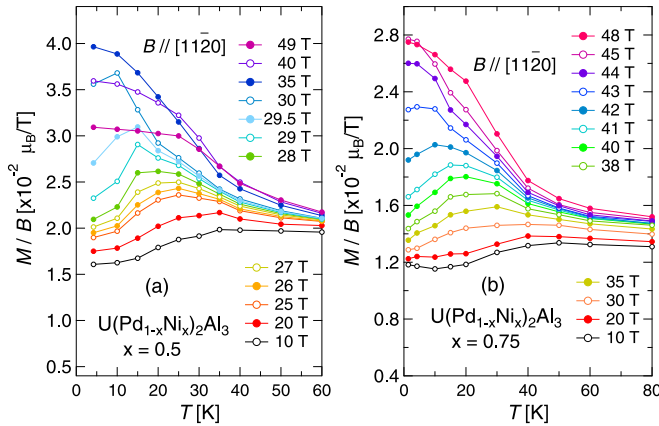


FIG. 5. The temperature dependence of the magnetization  $M(T)$  divided by each field  $B$  in  $\text{U}(\text{Pd}_{1-x}\text{Ni}_x)_2\text{Al}_3$  for (a)  $x = 0.5$  and (b)  $x = 0.75$ .

of the first-order nature of the MMT in  $\text{U}(\text{Pd}_{1-x}\text{Ni}_x)_2\text{Al}_3$  ( $x = 0.5$  and  $0.75$ ). It should also be noted that neither a phase transition nor anomaly is seen below the first-order MMT from our high-resolution magnetization measurements. With increasing  $T$ , the MMT becomes broader and finally disappears for both Ni concentrations.

Figures 5(a) and 5(b) show  $M(T)/B$  at various fields, obtained from the  $M(B)$  curves. As seen in the  $M(T)$  data, with increasing magnetic field, the susceptibility maximum  $T_{\chi_{\max}}(B)$  shifts to lower temperatures. Although the physical meaning of the susceptibility maximum remains unclear, it appears that the AF correlation (spin fluctuations) effect developing below  $T_{\chi_{\max}}$  is suppressed with increasing  $B$ .

Figure 6(a) shows the  $B$ - $T$  magnetic phase diagram of  $\text{U}(\text{Pd}_{0.5}\text{Ni}_{0.5})_2\text{Al}_3$  for  $B \parallel [11\bar{2}0]$  with a contour plot of magnetization  $M(T, B)$  [Fig. 4(a)], where the red region indicates the magnetic moment induced by the MMT. Here, we determine the MMT field  $B_m(T)$  to be the field of the peak in the derivative of the magnetization  $dM/dB$  [Fig. 6(b)]. The sharp peaks of  $dM/dB$  at 4.2 and 10 K indicate the first-order phase transition (solid diamonds) at  $B_m$ , as already seen in the clear step behavior at  $B_m$  in  $M(B)$ . It is noted that  $B_m$  slightly shifts to weaker fields when *below* 15 K but to stronger fields when *above* 15 K. We also show the AF transition temperature  $T_N(B)$  obtained from specific-heat  $C(T)$  measurements, which will be reported elsewhere in more detail. Specific-heat data suggest that the AF transition at  $T_N(B)$  is second order, and no phase transition is observed below the MMT, as seen in the  $M(B)$  curves [Figs. 4(a) and 4(b)]. In Fig. 6(a), although the behavior of the AF phase above 15 T is still unclear at present, it seems that the line of the second-order phase transition of  $T_N(B)$  meets the metamagnetic field  $B_m(T)$  (first order below  $T_N$ ) almost perpendicularly. In general, the line of second-order phase transition  $T_N(B)$  should not terminate at a critical end point, and the AF ordered phase is clearly distinguished from the PM state, possessing an order parameter. Our data and the obtained  $B$ - $T$  phase diagram suggest the presence of the tricritical point at  $T = 15$  K and  $B = 30$  T in  $\text{U}(\text{Pd}_{0.5}\text{Ni}_{0.5})_2\text{Al}_3$ , where the second-order phase transition is changed to the first-order one [red diamond in Fig. 6(a)]. Therefore, below  $T = 15$  K the MMT occurs just at the

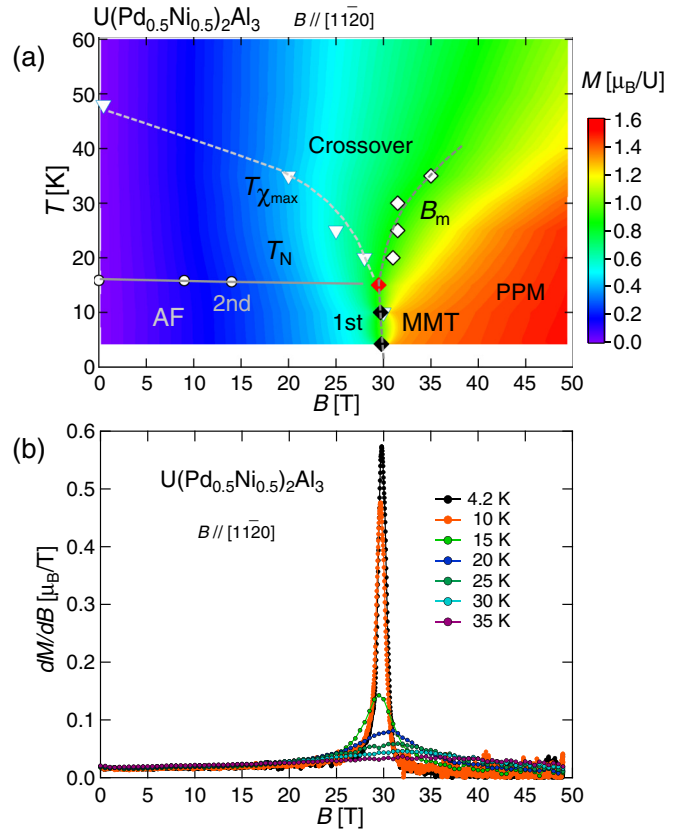


FIG. 6. (a) The  $B$ - $T$  phase diagram with the contour plot of magnetization  $M(T, B)$  of  $\text{U}(\text{Pd}_{0.5}\text{Ni}_{0.5})_2\text{Al}_3$  for  $B \parallel [11\bar{2}0]$ , where the lines are guides to the eyes. Here,  $B_m(T)$  was determined from the peak in  $dM/dB$ , and  $T_N(B)$  was obtained from the specific-heat measurements (raw data not shown).  $T_{\chi_{\max}}(B)$ , obtained from the  $M(T)$  data [Fig. 5(a)] is also plotted. (b)  $dM/dB$  in  $\text{U}(\text{Pd}_{0.5}\text{Ni}_{0.5})_2\text{Al}_3$  for  $B \parallel [11\bar{2}0]$ .

critical field of the AF order ( $B_m = B_c$ ). For  $x = 0.75$  the magnetic phase diagram is similar, although the first-order transition becomes broader than that for  $x = 0.5$ , presumably owing to disorder effects. The obtained magnetic phase diagram in the doped  $\text{U}(\text{Pd}_{1-x}\text{Ni}_x)_2\text{Al}_3$  is analogous to  $\text{UPd}_2\text{Al}_3$  [58,59].

It is noted that the MMT is observed in the PM state well above  $T_N$ , with  $B_m(T)$  shifting to higher fields with increasing  $T$  [Figs. 6(a) and 6(b)]. In addition, no field-induced phase transition is observed in  $dM(B)/dB$  data below  $B_m$  [Fig. 6(b)], suggesting that the MMT above  $T_N$  is a crossover anomaly without the symmetry change from the PM to polarized-paramagnetic (PPM) states in  $\text{U}(\text{Pd}_{1-x}\text{Ni}_x)_2\text{Al}_3$ . The occurrence of the crossover MMT from the PM to PPM states well above  $T_N$  [Fig. 6(b)] cannot be explained by the spin-flip transition of the localized AF ordered moments.

The observation of the MMT from the PM to PPM states (well above  $T_N$ ) may be consistent with the occurrence of a Lifshitz transition (without a change in symmetry) in  $\text{U}(\text{Pd}_{1-x}\text{Ni}_x)_2\text{Al}_3$ , but further experimental studies are necessary to prove this type of transition occurs. According to previous de Haas-van Alphen (dHvA) studies [60,61], which agree with band calculations [62,63], a change of the topology of the Fermi surface has been observed through the MMT



in  $\text{UPd}_2\text{Al}_3$ . However, the quantum oscillations in  $\text{UPd}_2\text{Al}_3$  have been observed at low temperatures ( $T \sim 30 \text{ mK} \ll T_N$ ). As the change in the Fermi surface should occur owing to the unfolding of the Brillouin zone, the dHvA measurements cannot be a demonstration of a Lifshitz transition in  $\text{UPd}_2\text{Al}_3$ . Recent thermoelectric power measurements may support the occurrence of a Lifshitz transition at  $B_m$  in  $\text{UPd}_2\text{Al}_3$  [64], but further studies are necessary to clarify this point for the isostructural system of  $\text{U}(\text{Pd}_{1-x}\text{Ni}_x)_2\text{Al}_3$ .

An important outcome of this study is the finding that the MMT is intimately connected with the AF correlation in  $\text{U}(\text{Pd}_{1-x}\text{Ni}_x)_2\text{Al}_3$ . As seen in Fig. 3(a), the energy scale of the MMT ( $B_m$  and  $T_{\chi_{\max}}$ ) becomes very large above  $x = 0.5$ , compared to the values of  $T_N$ . Nevertheless, for  $\text{UNi}_2\text{Al}_3$ , in which the Néel temperature is small ( $T = 4.1 \text{ K}$ ) compared to  $\text{UPd}_2\text{Al}_3$ , the AF order (spin-density-wave order) is robust in strong magnetic fields, and a decoupling of the AF order and the MMT does not occur in this compound; no phase transition was seen in  $dM/dB$  up to  $B_m$  for  $\text{UNi}_2\text{Al}_3$ . Here, it is noteworthy to compare  $\text{U}(\text{Pd}_{1-x}\text{Ni}_x)_2\text{Al}_3$  with  $\text{CeRu}_2\text{Si}_2$  and its doped systems. For  $\text{Ce}_{1-x}\text{La}_x\text{Ru}_2\text{Si}_2$  (above  $x = 0.08$ ) [29], it was reported that the low- $T$  ground state is an AF order and the MMT occurs as a first-order phase transition, analogous to  $\text{U}(\text{Pd}_{1-x}\text{Ni}_x)_2\text{Al}_3$ , although the MMT is a crossover anomaly in pure  $\text{CeRu}_2\text{Si}_2$ . Going to the pure  $\text{CeRu}_2\text{Si}_2$  lattice leads to a PM ground state, while a sharp crossover MMT occurs at  $B_m \sim 7.8 \text{ T}$ , caused by the drastic change in the Fermi surface [24]. A key point is that this MMT crossover occurs for a constant value of the magnetization in  $\text{CeRu}_2\text{Si}_2$  and its doped systems: it is considered that the magnetic polarization drives a Fermi surface reconstruction and thus a drastic change in the nature of the correlation.

As seen in Fig. 6(a), the crossover lines of  $T_{\chi_{\max}}(B)$  and  $B_m(T)$  meet at the tricritical point. As the low- $T$  ground state below  $T_N(B)$  is embedded into the lower-field region below  $T_{\chi_{\max}}(B)$ , it appears that AF fluctuations develop below  $T_{\chi_{\max}}(B)$ . This behavior implies that the MMT is caused by competition between the low-field AF regime and the PPM state. For  $\text{CeRu}_2\text{Si}_2$ , an inelastic neutron scattering study revealed a magnetic-field-induced FM correlation coupled to the MMT [31,32]. As no criticality in AF fluctuations appears on increasing magnetic field towards  $B_m$ , it is considered that the driving mechanism is the Lifshitz transition at  $B_m$  in  $\text{CeRu}_2\text{Si}_2$  [31]. Here, although the types of magnetic anisotropy are different between  $\text{U}(\text{Pd}_{1-x}\text{Ni}_x)_2\text{Al}_3$  (easy-plane anisotropy) and  $\text{CeRu}_2\text{Si}_2$  (strong Ising-type anisotropy) [21], the phenomena of susceptibility maximum and MMT occur for the easy-magnetization directions in the two aforementioned systems. By contrast, in the novel uranium superconductor  $\text{UTe}_2$ , the first-order MMT occurs when a magnetic field is applied along the hard-magnetization axis ( $H \parallel b$ ) [17–19], for which the broad maximum of magnetic susceptibility appears at around 35 K [65]. Interestingly, the reentrant superconductivity occurs for the hard-magnetization axis ( $H \parallel b$ ) [20]. It will be important to determine which type of AF fluctuation develops below  $T_{\chi_{\max}}(B)$  and to explore field-induced magnetic fluctuations in  $\text{U}(\text{Pd}_{1-x}\text{Ni}_x)_2\text{Al}_3$ , compared with those in  $\text{CeRu}_2\text{Si}_2$  and  $\text{UTe}_2$ .

Another interesting MMT system to compare with our results is  $\text{YbInCu}_4$ , which shows a first-order valence

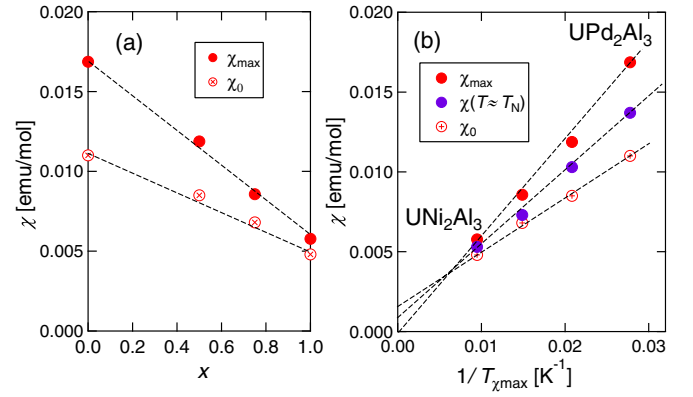


FIG. 7. (a)  $\chi_{\max}$  and low- $T$  susceptibility value  $\chi_0$  (the values linearly extrapolated to  $T = 0 \text{ K}$  below  $T_N$ ) in  $\text{U}(\text{Pd}_{1-x}\text{Ni}_x)_2\text{Al}_3$  as a function of Ni concentration  $x$  for  $B \parallel [11\bar{2}0]$ . (b)  $\chi_{\max}$ ,  $\chi(T \simeq T_N)$  (the susceptibility values in the PM state just above  $T_N$ ), and  $\chi_0$  as a function of  $1/T_{\chi_{\max}}$  in  $\text{U}(\text{Pd}_{1-x}\text{Ni}_x)_2\text{Al}_3$ . Here, the dashed linear lines are guides to the eye.

transition at  $T_v = 42 \text{ K}$  [66,67]. In this compound, the first-order MMT occurs together with a valence transition at a magnetic field  $B_v$ . Interestingly, the obtained relation of  $B_m(x)$  and  $T_{\chi_{\max}}(x)$  for  $\text{U}(\text{Pd}_{1-x}\text{Ni}_x)_2\text{Al}_3$  is reminiscent of an empirical linear relation between  $B_v(x)$  and  $T_v(x)$  in  $\text{YbIn}_{1-x}\text{Ag}_x\text{Cu}_4$  [68,69], although the transition at  $T_v(x)$  in  $\text{YbIn}_{1-x}\text{Ag}_x\text{Cu}_4$  is first order, unlike the crossover anomaly at  $T_{\chi_{\max}}(x)$  in  $\text{U}(\text{Pd}_{1-x}\text{Ni}_x)_2\text{Al}_3$ . It should be noted, however, that the nature of the  $B$ - $T$  phase diagram is clearly distinguished between  $\text{U}(\text{Pd}_{1-x}\text{Ni}_x)_2\text{Al}_3$  and  $\text{YbInCu}_4$ ; while the tricritical point is present in the  $B$ - $T$  phase diagram for  $\text{U}(\text{Pd}_{1-x}\text{Ni}_x)_2\text{Al}_3$ , the MMT is always first order in the doped  $\text{YbIn}_{1-x}\text{Ag}_x\text{Cu}_4$  and the pure system under high pressures [67]. Additionally, unlike  $\text{U}(\text{Pd}_{1-x}\text{Ni}_x)_2\text{Al}_3$ , the MMT does not occur from the PM to PPM states in  $\text{YbIn}_{1-x}\text{Ag}_x\text{Cu}_4$ , suggesting that the MMT is governed by different origins in the above Yb and U systems.

Finally, we examine the relation between the magnetic susceptibility ( $\chi_{\max}$  and the low- $T$  value  $\chi_0$ ) and  $T_{\chi_{\max}}$ . Here, the value of  $\chi_0$  is the value of magnetic susceptibility linearly extrapolated to  $T = 0 \text{ K}$ , which is also the initial slope of the magnetization curve  $M(B)$  ( $B \ll B_m$ ) at  $T = 0 \text{ K}$ . Figure 7(a) shows the Ni concentration evolution of  $\chi_{\max}(x) \equiv \chi(T_{\chi_{\max}}, x)$  and  $\chi_0(x)$ . The decrease in  $\chi_{\max}$  and  $\chi_0$  is roughly linear in  $x$  [Fig. 7(a)]. Figure 7(b) shows  $\chi_{\max}$ ,  $\chi(T \simeq T_N)$ , and  $\chi_0$  as a function of  $1/T_{\chi_{\max}}$  for  $\text{U}(\text{Pd}_{1-x}\text{Ni}_x)_2\text{Al}_3$ , where  $\chi(T \simeq T_N)$  is defined as the susceptibility value in the PM state just above  $T_N$ . Interestingly, as seen in Fig. 7(b),  $\chi_{\max}$ ,  $\chi(T \simeq T_N)$ , and  $\chi_0$  are proportional to  $1/T_{\chi_{\max}}$ . Using the relation  $B_m \propto T_{\chi_{\max}}$ , we find a roughly linear relation of  $\chi_{\max} \propto \chi(T \simeq T_N) \propto \chi_0 \propto 1/T_{\chi_{\max}} \propto 1/B_m$ . The relation  $\chi_0 \propto 1/B_m$  implies that the magnetization at the onset of the MMT is roughly independent of  $x$ , as  $\chi_0$  is the initial slope of the  $M(B)$  curve at low temperatures. As seen in Fig. 2(a), owing to the large nonlinear susceptibility below  $B_m$ , the values of  $M_0 \sim \chi_0 B_m$  slightly change with increasing  $x$ . It is noted that the magnetization value at the midpoint of the MMT is almost unchanged ( $\sim 0.9 \mu_B/\text{U}$ ). As seen in Fig. 4(a), the  $M(B)$  curves for 4.2 and 15 K ( $\sim T_N \sim T_{\text{Cr}}$ ) cross each other at around the midpoint

of the MMT. As the line of  $T_N(B)$  is perpendicular to  $B_m(T)$  in the  $B$ - $T$  phase diagram, the magnetization at the midpoint of the MMT is roughly estimated to be the critical value at the tricritical point [ $M_{cr} = \chi(T = T_{cr})B_m \sim \chi(T \simeq T_N)B_m$ ].

As reported previously for polycrystalline samples of  $U(\text{Pd}_{1-x}\text{Ni}_x)_2\text{Al}_3$ , the entropy for a  $5f$  electron at around the temperature of susceptibility maximum  $T_{\chi_{\max}}(x)$  is almost constant for whole Ni concentrations [ $S_{5f}(T_{\chi_{\max}}) = \text{const}$ ] [57], while the magnetic entropy  $S_{5f}(T_N)$  at  $T_N(x)$  significantly decreases with increasing  $x$ ;  $S_{5f}(T_N) = 0.16R$  and  $0.01R$  for  $x = 0$  and  $x = 1$ , respectively [70]. At  $T_{\chi_{\max}}$ , the free energy of thermally fluctuating AF moments of  $5f$  electrons is roughly estimated to be  $-T_{\chi_{\max}}S_{5f}(T_{\chi_{\max}})$ . The MMT probably occurs when the Zeeman energy of the magnetic polarization ( $-M_{cr}B$ ) approaches the free energy of  $-T_{\chi_{\max}}S_{5f}(T_{\chi_{\max}})$ . Therefore, it appears that the MMT in  $U(\text{Pd}_{1-x}\text{Ni}_x)_2\text{Al}_3$  is dominated by the unchanged threshold [ $M_{cr} = \frac{T_{\chi_{\max}}}{B_m}S_{5f}(T_{\chi_{\max}})$ ], although the energy scale of the AF correlation effect that develops below  $T_{\chi_{\max}}$  becomes larger with increasing Ni doping. As pointed out previously, similar behavior was reported in  $\text{CeRu}_2\text{Si}_2$  under high pressure [71]: again, the MMT is driven by a critical value of the magnetization. Here, the saturated magnetic moment above  $B_m$  and the discontinuity of magnetization  $\Delta M$  are reduced in  $U(\text{Pd}_{1-x}\text{Ni}_x)_2\text{Al}_3$  with increasing  $x$  ( $x = 0, 0.5$ , and  $0.75$ ); the understanding of this behavior is left for future study.

#### IV. SUMMARY

In summary, our high-resolution magnetization measurements up to 90 T using single-crystalline samples have revealed the occurrence of the MMT in pure  $\text{UNi}_2\text{Al}_3$  as well as doped  $U(\text{Pd}_{1-x}\text{Ni}_x)_2\text{Al}_3$ . For  $x = 0.5$  and  $0.75$ , the observed  $M(B)$  curves show a sharp step at the MMT field  $B_m$ , providing a strong indication of its first-order

nature. The MMT is still observed above  $T_N$  as a crossover anomaly with no symmetry change, suggesting that the MMT in  $U(\text{Pd}_{1-x}\text{Ni}_x)_2\text{Al}_3$  is not explained by the conventional spin flip of AF localized moments. The obtained magnetic phase diagram for  $x = 0.5$  suggests the presence of a tricritical point in  $U(\text{Pd}_{1-x}\text{Ni}_x)_2\text{Al}_3$ , analogous to  $\text{UPd}_2\text{Al}_3$ . The first-order MMT may occur owing to the competition between the field-induced new instability and the AF regime for  $T < T_N(B) < T_{\chi_{\max}}$ . We found the scaling behavior of  $\chi(T/T_{\max})/\chi_{\max} = f(T/T_{\chi_{\max}})$  and the linear relation of  $B_m(x) \propto T_{\chi_{\max}}(x)$ ; the MMT is linearly scaled by the energy scale of AF spin fluctuations developing below  $T_{\chi_{\max}}$  with Ni doping. Whereas the magnetic susceptibility is strongly suppressed with increasing  $x$ , the obtained relation of  $\chi_{\max} \propto \chi_0 \propto 1/T_{\max}$  indicates that the critical value of the magnetic polarization at the MMT is almost unchanged in  $U(\text{Pd}_{1-x}\text{Ni}_x)_2\text{Al}_3$ .

#### ACKNOWLEDGMENTS

We greatly appreciate K. Suzuki's technical support in the use of the energy dispersive x-ray spectrometer at the Oarai facility at Tohoku University. We would also like to thank T. Sakakibara, A. Miyake, H. Amitsuka, N. Tateiwa, Y. Haga, A. Pourret, M. Yokoyama, Y. Matsumoto, Y. Ikeda, S. Hoshino, A. Nakamura, and A. Maurya for valuable discussions. K.M. was supported by the Japan Society for the Promotion of Science through the Program for Leading Graduate Schools (MERIT). This work is supported in part by KAKENHI (Grants No. JP15H05884, No. JP15H05882, No. JP15H05745, No. JP16H04006, No. JP17K14328). Y.S. would like to acknowledge all the support from Institute for Materials Research, Tohoku University in growing monocrystalline uranium samples using the joint research facility at Oarai.

- 
- [1] E. Strykowski and N. Gojordano, *Adv. Phys.* **26**, 487 (1977).  
 [2] T. Sakakibara, T. Goto, K. Yoshimura, and K. Fukamichi, *J. Phys.: Condens. Matter* **2**, 3381 (1990).  
 [3] T. Sakakibara, T. Goto, K. Yoshimura, K. Murata, and K. Fukamichi, *J. Magn. Magn. Mater.* **90-91**, 131 (1990).  
 [4] P. Fazekas, *Lecture Notes on Electron Correlation and Magnetism* (World Scientific, Singapore, 1999).  
 [5] H. Yamada, *Phys. Rev. B* **47**, 11211 (1993).  
 [6] S.-I. Ikeda, Y. Maeno, S. Nakatsuji, M. Kosaka, and Y. Uwatoko, *Phys. Rev. B* **62**, R6089 (2000).  
 [7] R. S. Perry, L. M. Galvin, S. A. Grigera, L. Capogna, A. J. Schofield, A. P. Mackenzie, M. Chiao, S. R. Julian, S. I. Ikeda, S. Nakatsuji, Y. Maeno, and C. Pfleiderer, *Phys. Rev. Lett.* **86**, 2661 (2001).  
 [8] S. A. Grigera, P. Gegenwart, R. A. Borzi, F. Weickert, A. J. Schofield, R. S. Perry, T. Tayama, T. Sakakibara, Y. Maeno, A. G. Green, and A. P. Mackenzie, *Science* **306**, 1154 (2004).  
 [9] W. Wu, A. McCollam, S. A. Grigera, R. S. Perry, A. P. Mackenzie, and S. R. Julian, *Phys. Rev. B* **83**, 045106 (2011).  
 [10] D. Sun, A. W. Rost, R. S. Perry, A. P. Mackenzie, and M. Brando, *Phys. Rev. B* **97**, 115101 (2018).  
 [11] M. Jaime, K. H. Kim, G. Jorge, S. McCall, and J. A. Mydosh, *Phys. Rev. Lett.* **89**, 287201 (2002).  
 [12] N. Harrison, M. Jaime, and J. A. Mydosh, *Phys. Rev. Lett.* **90**, 096402 (2003).  
 [13] W. Knafo, F. Duc, F. Bourdarot, K. Kuwahara, H. Nojiri, D. Aoki, J. Billette, P. Frings, X. Tonon, E. Lelièvre-Berna, J. Flouquet, and L.-P. Regnault, *Nat. Commun.* **7**, 13075 (2016).  
 [14] J. A. Mydosh and P. M. Oppeneer, *Philos. Mag.* **94**, 3642 (2014).  
 [15] S. Ran, C. Eckberg, Q.-P. Ding, Y. Furukawa, T. Metz, S. R. Saha, I.-L. Liu, M. Zic, H. Kim, J. Paglione, and N. P. Butch, *Science* **365**, 684 (2019).  
 [16] D. Aoki, A. Nakamura, F. Honda, D. X. Li, Y. Homma, Y. Shimizu, Y. J. Sato, G. Knebel, J.-P. Brison, A. Pourret, D. Braithwaite, G. Lapertot, Q. Niu, M. Vališka, H. Harima, and J. Flouquet, *J. Phys. Soc. Jpn.* **88**, 043702 (2019).  
 [17] A. Miyake, Y. Shimizu, Y. J. Sato, D. X. Li, A. Nakamura, Y. Homma, F. Honda, J. Flouquet, M. Tokunaga, and D. Aoki, *J. Phys. Soc. Jpn.* **88**, 063706 (2019).  
 [18] S. Ran, I.-L. Liu, Y. S. Eo, D. J. Campbell, P. M. Neves, W. T. Fuhrman, S. R. Saha, C. Eckberg, H. Kim, D. Graf,

- F. Balakirev, J. Singleton, J. Paglione, and N. P. Butch, *Nat. Phys.* (2019), doi:[10.1038/s41567-019-0670-x](https://doi.org/10.1038/s41567-019-0670-x).
- [19] W. Knafo, M. Vališka, D. Braithwaite, G. Lapertot, G. Knebel, A. Pourret, J.-P. Brison, J. Flouquet, and D. Aoki, *J. Phys. Soc. Jpn.* **88**, 063705 (2019).
- [20] G. Knebel, W. Knafo, A. Pourret, Q. Niu, M. Vališka, D. Braithwaite, G. Lapertot, M. Nardone, A. Zitouni, S. Mishra, I. Sheikin, G. Seyfarth, J.-P. Brison, D. Aoki, and J. Flouquet, *J. Phys. Soc. Jpn.* **88**, 063707 (2019).
- [21] P. Haen, J. Flouquet, F. Lapiere, P. Lajay, and G. Remenyi, *J. Low. Temp. Phys.* **67**, 391 (1987).
- [22] H. Aoki, S. Uji, A. K. Albessard, and Y. Onuki, *Phys. Rev. Lett.* **71**, 2110 (1993).
- [23] T. Sakakibara, T. Tayama, K. Matsuhira, H. Mitamura, H. Amitsuka, K. Maezawa, and Y. Onuki, *Phys. Rev. B* **51**, 12030(R) (1995).
- [24] J. Flouquet, P. Haen, S. Raymond, D. Aoki, and G. Knebel, *Phys. B (Amsterdam, Neth.)* **319**, 251 (2002).
- [25] K. Miyake and H. Ikeda, *J. Phys. Soc. Jpn.* **75**, 033704 (2006).
- [26] R. Daou, C. Bergemann, and S. R. Julian, *Phys. Rev. Lett.* **96**, 026401 (2006).
- [27] M. Boukahil, A. Pourret, G. Knebel, D. Aoki, Y. Onuki, and J. Flouquet, *Phys. Rev. B* **90**, 075127 (2014).
- [28] R. A. Fisher, C. Marcenat, N. E. Phillips, P. Haen, F. Lapiere, P. Lajay, J. Flouquet, and J. Voiron, *J. Phys. Temp. Phys.* **84**, 49 (1991).
- [29] D. Aoki, C. Paulsen, T. D. Matsuda, L. Malone, G. Knebel, P. Haen, P. Lajay, R. Settai, Y. Onuki, and J. Flouquet, *J. Phys. Soc. Jpn.* **80**, 053702 (2011).
- [30] D. Aoki, C. Paulsen, H. Kotegawa, F. Hardy, C. Meingast, P. Haen, M. Boukahil, W. Knafo, E. Ressouche, S. Raymond, and J. Flouquet, *J. Phys. Soc. Jpn.* **81**, 034711 (2012).
- [31] S. Raymond, L. P. Regnault, S. Kambe, J. Flouquet, and P. Lajay, *J. Phys.: Condens. Matter* **10**, 2363 (1998).
- [32] M. Sato, Y. Koike, S. Katano, N. Metoki, H. Kadowaki, and S. Kawarazaki, *J. Phys. Soc. Jpn.* **73**, 3418 (2004).
- [33] A. de Visser, F. de Boer, A. A. Menovsky, and J. J. M. Franse, *Solid State Commun.* **64**, 527 (1987).
- [34] J. J. M. Franse, H. P. van der Meulen, A. A. Menovsky, A. de Visser, J. A. A. J. Perenboom, and H. van Kempen, *J. Magn. Mater.* **90-91**, 29 (1990).
- [35] A. de Visser, H. Nakotte, L. T. Tai, A. A. Menovsky, S. A. M. Mentink, G. J. Nieuwenhuys, and J. A. Mydosh, *Phys. B (Amsterdam, Neth.)* **179**, 84 (1992).
- [36] K. Sugiyama, T. Inoue, T. Ikeda, N. Sato, T. Komatsubara, A. Yamagishi, and M. Date, *Phys. B (Amsterdam, Neth.)* **186-188**, 723 (1993).
- [37] K. Oda, T. Kumada, K. Sugiyama, N. Sato, T. Komatsubara, and M. Date, *J. Phys. Soc. Jpn.* **63**, 3115 (1994).
- [38] N. V. Mushnikov, T. Goto, K. Kamishima, H. Yamada, A. V. Andreev, Y. Shiokawa, A. Iwao, and V. Sechovsky, *Phys. Rev. B* **59**, 6877 (1999).
- [39] D. Aoki, T. Combier, V. Taufour, T. D. Matsuda, G. Knebel, H. Kotegawa, and J. Flouquet, *J. Phys. Soc. Jpn.* **80**, 094711 (2011).
- [40] N. Kimura, N. Kabeya, H. Aoki, K. Ohyama, M. Maeda, H. Fujii, M. Kogure, T. Asai, T. Komatsubara, T. Yamamura, and I. Satoh, *Phys. Rev. B* **92**, 035106 (2015).
- [41] Y. Shimizu, D. Braithwaite, B. Salce, T. Combier, D. Aoki, E. N. Hering, S. M. Ramos, and J. Flouquet, *Phys. Rev. B* **91**, 125115 (2015).
- [42] M. Brando, D. Belitz, F. M. Grosche, and T. R. Kirkpatrick, *Rev. Mod. Phys.* **88**, 025006 (2016).
- [43] C. Geibel, C. Schank, S. Thies, H. Kitazawa, C. D. Bredl, A. Biihm, M. Rau, A. Grauel, R. Caspary, R. Helfrich, U. Ahlheim, G. Weber, and F. Steglich, *Z. Phys. B* **84**, 1 (1991).
- [44] C. Geibel, S. Thies, D. Kaczorowski, A. Mehner, A. Grauel, B. Seidel, U. Ahlheim, R. Helfrich, K. Petersen, C. D. Bredl, and F. Steglich, *Z. Phys. B* **83**, 305 (1991).
- [45] A. Krimmel, P. Fischer, B. Roessli, H. Maletta, C. Geibel, C. Schank, A. Grauel, A. Loidl, and F. Steglich, *Z. Phys. B* **86**, 161 (1992).
- [46] A. Hiess, N. Bernhoeft, N. Metoki, G. H. Lander, B. Roessli, N. K. Sato, N. Aso, Y. Haga, Y. Koike, T. Komatsubara, and Y. Onuki, *J. Phys.: Condens. Matter* **18**, R437 (2006).
- [47] A. Schroder, J. G. Lussier, B. D. Gaulin, J. D. Garrett, W. J. L. Buyers, L. Rebelsky, and S. M. Shapiro, *Phys. Rev. Lett.* **72**, 136 (1994).
- [48] J. G. Lussier, M. Mao, A. Schröder, J. D. Garrett, B. D. Gaulin, S. M. Shapiro, and W. J. L. Buyers, *Phys. Rev. B* **56**, 11749 (1997).
- [49] B. D. Gaulin, M. Mao, C. R. Wiebe, Y. Qiu, S. M. Shapiro, C. Broholm, S.-H. Lee, and J. D. Garrett, *Phys. Rev. B* **66**, 174520 (2002).
- [50] D. Aoki, W. Knafo, and I. Sheikin, *C. R. Phys.* **14**, 53 (2013).
- [51] H. Nakotte, K. Bakker, Z. Koziol, F. R. de Boer, and A. V. Andreev, *IEEE Trans. Mag.* **30**, 1199 (1994).
- [52] N. Sato, N. Koga, and T. Komatsubara, *J. Phys. Soc. Jpn.* **65**, 1555 (1996); N. Sato, N. Aso, N. Tateiwa, N. Koga, T. Komatsubara, and N. Metoki, *Phys. B (Amsterdam, Neth.)* **230-232**, 367 (1997).
- [53] A. Grauel, A. Böhm, H. Fischer, C. Geibel, R. Kohler, R. Modler, C. Schank, F. Steglich, G. Weber, T. Komatsubara, and N. Sato, *Phys. Rev. B* **46**, 5818 (1992).
- [54] C. Geibel, A. Böhm, R. Caspary, K. Gloos, A. Grauel, P. Hellmann, R. Modler, C. Schank, G. Weber, and F. Steglich, *Phys. B (Amsterdam, Neth.)* **186-188**, 188 (1993).
- [55] S. Takeyama, R. Sakakura, Y. H. Matsuda, A. Miyata, and M. Tokunaga, *J. Phys. Soc. Jpn.* **81**, 014702 (2012).
- [56] C. Schank, F. Jährling, A. Grauel, R. Borth, R. Helfrich, T. Lühmann, P. H. P. Reinders, C. Geibel, and F. Steglich, *J. Alloys Compd.* **213-214**, 509 (1994).
- [57] C. Schank, F. Jährling, U. Tegel, C. Geibel, A. Grauel, A. Böhm, R. Borth, R. Helfrich, D. Jaeckel, G. Weber, and F. Steglich, *International Conference on the Physics of Transition Metals*, edited by P. M. Oppeneer and J. Kübler, Vol. I (World Scientific, Darmstadt, Germany, 1992).
- [58] K. Sugiyama, M. Nakashima, M. Futoh, H. Ohkuni, T. Inoue, K. Kindo, N. Kimura, E. Yamamoto, Y. Haga, T. Honma, R. Settai, and Y. Onuki, *Phys. B (Amsterdam, Neth.)* **281-282**, 244 (2000).
- [59] J. S. Kim, N. K. Sato, and G. R. Stewart, *J. Low. Temp. Phys.* **124**, 527 (2001).
- [60] Y. Inada, H. Yamagami, Y. Haga, K. Sakurai, Y. Tokiwa, T. Honma, E. Yamamoto, Y. Onuki, and T. Yanagisawa, *J. Phys. Soc. Jpn.* **68**, 3643 (1999); Y. Haga, Y. Inada, K. Sakurai, Y.

- Tokiwa, E. Yamamoto, T. Honma, and Y. Onuki, *ibid.* **68**, 342 (1999).
- [61] T. Terashima, C. Haworth, M. Takashita, H. Aoki, N. Sato, and T. Komatsubara, *Phys. Rev. B* **55**, R13369 (1997).
- [62] L. M. Sandratskii, J. Kübler, P. Zahn, and I. Mertig, *Phys. Rev. B* **50**, 15834 (1994).
- [63] K. Knöpfle, A. Mavromaras, L. M. Sandratskii, and J. Kübler, *J. Phys.: Condens. Matter* **8**, 901 (1996).
- [64] A. Gourgout, Ph.D. thesis, CEA-Grenoble, Université Grenoble Alpes, 2017.
- [65] S. Ikeda, H. Sakai, D. Aoki, Y. Homma, E. Yamamoto, A. Nakamura, Y. Shiokawa, Y. Haga, and Y. Onuki, *J. Phys. Soc. Jpn. Suppl.* **75**, 116 (2006).
- [66] I. Felner and I. Nowik, *Phys. Rev. B* **33**, 617 (1986).
- [67] C. D. Immer, J. L. Sarrao, Z. Fisk, A. Lacerda, C. Mielke, and J. D. Thompson, *Phys. Rev. B* **56**, 71 (1997).
- [68] H. A. Katori, T. Goto, and K. Yoshimura, *Phys. B (Amsterdam, Neth.)* **201**, 159 (1994).
- [69] J. L. Sarrao, C. D. Immer, C. L. Benton, Z. Fisk, J. M. Lawrence, D. Mandrus, and J. D. Thompson, *Phys. Rev. B* **54**, 12207 (1996).
- [70] We also checked specific heat  $C(T)$  for single-crystalline  $U(Pd_{1-x}Ni_x)_2Al_3$ , and our results were in good agreement with the previous reports [57].
- [71] J.-M. Mignot, J. Flouquet, P. Haen, F. Lapierre, L. Puech, and J. Voiron, *J. Magn. Magn. Mater.* **76-77**, 97 (1988).